Articles

Electron Paramagnetic Resonance Studies of a *ras* p21-Mn^{II}GDP Complex in Solution†

David G. Latwesen,‡ Martin Poe,§ John S. Leigh,∥ and George H. Reed*,‡

Institute for Enzyme Research, Graduate School, and Department of Biochemistry, College of Agricultural and Life Sciences, University of Wisconsin, Madison, Wisconsin 53705, Merck Sharp & Dohme Research Laboratories, Rahway, New Jersey 07065, and Department of Radiology, University of Pennsylvania School of Medicine, Philadelphia, Pennsylvania 19104

Received January 30, 1992; Revised Manuscript Received March 19, 1992

ABSTRACT: The number of water molecules bound to Mn^{2+} in the complex with a variant of Ha *ras* p21 and GDP has been determined by electron paramagnetic resonance (EPR) measurements in ^{17}O-enriched water. A resolution enhancement method has been used to improve quantitation of the spectral data. These spectroscopic measurements show that Mn^{2+} has four water ligands in this complex, a result in agreement with the conclusions of a previous paper [Smithers, G. W., Poe, M., Latwesen, D. G., & Reed, G. H. (1990) *Arch. Biochem. Biophys. 280*, 416-420]. The resolution enhancement method has also been applied in a measurement of the ^{17}O-Mn^{2+} superhyperfine coupling constant of ^{17}O in the β-phosphate of the GDP in the *ras* p21 complex. The intrinsically narrow EPR signals of Mn^{2+} in the complex with *ras* p21 and GDP in ^2H_2O respond to resolution enhancement such that the superhyperfine splitting from the ^{17}O nuclear spin ($I = {}^5/_2$) becomes visible in the EPR signals. An ^{17}O-Mn^{2+} superhyperfine coupling constant is obtained from simulation of the resolution-enhanced EPR spectrum.

Crystallographic studies of the Ha *ras* p21 proteins have provided detailed views of the binding site for the metal-guanine nucleotide complex and of changes in the structure when the bound GDP is replaced by analogues of GTP that are resistant to hydrolysis (Milburn et al., 1990; Tong et al., 1991; Schlichting et al., 1990; Pai et al., 1990). This structural transition, called a "molecular switch", is vital to the proposed signal-transducing function of the protein (Barbacid, 1987). The nucleotide binding domain of the *ras* p21 proteins shares significant sequence homology with regions of the larger class of G proteins (Hall, 1990) and with regions of other proteins that bind nucleotides such as cAMP-dependent protein kinase, F_1-ATPase, adenylate kinase, myosin, RecA, a superfamily of "ATP-binding-cassette" transport proteins, and the cystic fibrosis gene product (Fry et al., 1986; Ames, 1986; Hyde et al., 1990). The presence of these sequence homologies (or nucleotide binding cassettes) suggests similarities in binding sites for metal-nucleotides among diverse proteins. Moreover, changes in protein structure associated with the hydrolysis and departure of the terminal phosphate group of a bound nucleoside triphosphate are believed to be crucial to the biological functions of many of the same proteins. Thus, the nucleotide-dependent structural transition of the p21 proteins may be prototypic of those associated with other nucleoside triphosphate hydrolases.

The conformational transition of the *ras* p21 protein is propagated from the immediate vicinity of the γ-phosphate group to regions some 40 Å distant from this locus and involves ligand exchanges in the primary coordination sphere of the bound Mg^{2+} ion (Pai et al., 1989; Milburn et al., 1990; Tong et al., 1991; Schlichting et al., 1990). In addition to the loss of the γ-phosphate as a ligand upon conversion of GTP to GDP, the hydroxyl group of Thr-35, which is a ligand for Mg^{2+} in the triphosphate state, relinquishes its position to a water molecule. The orientation of Thr-35 appears to govern the conformation of loop 2 which has been termed the "switch I region" of the molecule (Milburn et al., 1990). The hydroxyl group of Ser-17 is also a ligand for the Mg^{2+}, but this liganding interaction remains static in the GDP and GTP states. There are two different views regarding the occurrence of additional metal-ligand exchanges in the switch transition. When the GDP state is created within the crystal by photolysis and subsequent hydrolysis of a caged form of GTP, the Mg^{2+} appears to lose an intervening water ligand and acquire the carboxylate of Asp-57 as a ligand (Schlichting et al., 1990). However, because the GDP is generated in situ and the molecule undergoes a significant structural transition upon this conversion, crystal contacts may have perturbed the structure of the product GDP complex (Wittinghofer & Pai, 1991). On the other hand, crystallographic analysis of crystals obtained from solutions of the *ras* p21 complex with MgGDP indicates that the hydroxyl of Ser-17 is the only first-sphere ligand to Mg^{2+} that is contributed by the protein (Milburn et al., 1990; Tong et al., 1991).

The two models of metal ion coordination in the *ras* p21-GDP complex differ with respect to the number of water molecules bound to the metal ion. Three water ligands are present if Asp-57 binds directly, whereas four water ligands are present if Asp-57 remains in the second sphere. In a previous paper, electron paramagnetic resonance (EPR)[1]

† This work was supported by Grants GM35752 (G.H.R.) and RR02305 (J.S.L.) from NIH.

* Address correspondence to this author at the Institute for Enzyme Research, University of Wisconsin, 1710 University Ave., Madison, WI 53705.

‡ University of Wisconsin.

§ Merck Sharp & Dohme Research Laboratories.

∥ University of Pennsylvania School of Medicine.

[1] Abbreviations: EPR, electron paramagnetic resonance; NMR, nuclear magnetic resonance; S/N, signal-to-noise ratio.

0006-2960/92/0431-4946$03.00/0

measurements in $H_2{}^{17}O$-enriched solvent were used to estimate the hydration number of Mn^{2+} in the $Mn^{II}GDP$ complexes with three variants of Ha *ras* p21 (Smithers et al., 1990). The ^{17}O-induced inhomogeneous broadening in the EPR signals from complexes in ^{17}O-enriched water was modeled most satisfactorily with four sites for water in the first coordination sphere. The distinction between the three and four water models was, however, less conspicuous than that between models of two and three water ligands.

Intense biological interest in the details of the molecular switch function of the *ras* p21–metal–nucleotide species, the prevalence of the nucleotide binding cassette sequences, and the apparent uncertainty in the state of coordination of Asp-57 prompted an attempt to determine, with higher confidence, the hydration number of Mn^{2+} in the *ras* p21–$Mn^{II}GDP$ complex in the solution phase by EPR spectroscopy. In this paper, resolution enhancement of the EPR signals using Fourier transforms and convolution methods has been employed to improve the contrast between the three and four water ligand possibilities and to quantitate the ^{17}O–Mn^{2+} superhyperfine coupling interaction.

Experimental Procedures

Materials. The *ras* p21 protein used in these studies, *ras* $p21_{EJ}$, is a variant of Harvey-*ras* p21 (Gibbs et al., 1984; Ellis et al., 1982) with Val at position 12 and Thr at position 59 in the p21 sequence. The protein was purified and characterized as described previously (Smithers et al., 1990). For EPR experiments, 0.5–0.7 μmol of protein was dialyzed for 6 h at 4 °C versus 100 volumes of 0.1 M NaCl, 0.05 Tris-HCl, pH 7.5, 5 mM dithiothreitol, 0.01% (w/v) *n*-octyl β-glucopyranoside, and 0.03 mM GDP (buffer A) with 1 mM EDTA. The protein was then dialyzed for 94 h versus 150 volumes, of buffer A without EDTA. Solutions of the dialyzed protein were concentrated to 1.0 mL by ultrafiltration with an Amicon PM-10 membrane. $MnSO_4$ (0.7 mol/mol of p21) in dialysis buffer was added, and the solution was lyophilized to dryness. The GTPase activities of the protein recovered fully after lyophilization and dissolution.

For measurements of the *ras* p21 complex in $H_2{}^{17}O$-enriched solvent, lyophilized samples of protein and buffer components were dissolved in a stock solution, and four aliquots were lyophilized and redissolved either in normal water or in water enriched in $H_2{}^{17}O$ (41%; Miles Laboratories).

β-^{17}O-Enriched GDP and also unlabeled GDP were prepared as described by Eccleston et al. (1981). These nucleotides contained some unidentified contaminant that copurified with GDP during anion-exchange chromatography and interfered with the EPR measurements. This contaminant was removed by a procedure similar to that described by Eccleston et al. (1981). GDP was first converted to GTP with a pyruvate kinase/nucleoside diphosphokinase coupled reaction (Scheme I). The GTP was purified by anion-exchange chromatography and converted back to GDP with a nucleoside diphosphokinase/hexokinase coupled reaction (Scheme II).

Scheme I

$$\text{GDP + ATP (trace)} \xrightarrow{\text{NDPK}} \text{GTP + ADP (trace)}$$

$$\text{P-enolpyruvate + ADP (trace)} \xrightarrow{\text{PK}} \text{pyruvate + ATP (trace)}$$

Scheme II

$$\text{GTP + ADP (trace)} \xrightarrow{\text{NDPK}} \text{GDP + ATP (trace)}$$

$$\text{glucose + ATP (trace)} \xrightarrow{\text{HK}} \text{glucose-6-P + ADP (trace)}$$

The solution for the nucleoside diphosphokinase/pyruvate kinase coupled reaction was prepared as described by Eccleston et al. (1981), and the solution for the nucleoside diphosphokinase/hexokinase coupled reaction contained 10 mM Tris-HCl, pH 8.0, 3.5 mM GTP, 10 mM $MgCl_2$, 40 mM glucose, 0.02 mM ADP, 40 units of yeast hexokinase (obtained from Boehringer Mannheim Biochemicals as an ammonium sulfate suspension and dialyzed exhaustively against 0.1 M KCl/10 mM Tris-HCl, pH 8.0, to remove any EDTA present in the storage buffer), and 4 units of nucleoside diphosphokinase (Sigma).

Samples of the *ras* p21–Mn^{II}[β-^{17}O]GDP complex and a matched sample with unlabeled GDP were prepared by adding 0.16 μmol of either β-^{17}O-enriched GDP or GDP to matched stock solutions (containing 0.06 μmol of bound GDP) and *ras* p21 in buffer A. These solutions were incubated at 4 °C overnight to permit exchange of added β-^{17}O-enriched GDP with GDP already present in the protein. The samples were then lyophilized to dryness and redissolved in 6 μL of ^2H_2O.

EPR Measurements. EPR spectra were obtained at 35 GHz with a Varian E-109Q spectrometer. The spectrometer was interfaced to an IBM-AT microcomputer for data acquisition. For convenience in programming, the spectral data were exported to a VAX workstation for subsequent off-line processing. Samples were contained in quartz capillary tubes (Reed & Markham, 1984), and the temperature was maintained by a steady flow of dry N_2 in a standard Varian flow dewar.

Spectral Subtraction Method. The spectral subtraction method has been described in detail previously (Reed & Leyh, 1980; Smithers et al., 1990; Lodato & Reed, 1987), and a brief summary is provided here. In samples with less than 100% enrichment in ^{17}O, the experimentally observed EPR spectra consist of concentration-weighted superpositions of signals from complexes in which Mn^{2+} is bound exclusively to nonmagnetic isotopes of oxygen (i.e., ^{16}O and ^{18}O) and broader signals from complexes in which Mn^{2+} is bound to one or more ^{17}O ligands. The relative contribution of each type of signal to the observed EPR signal is a function of the ^{17}O enrichment in the ligand, $f(^{17}O)$, and the number of coordination sites, n, occupied by the ligand. For example, the fractional contribution from the signal deriving from Mn^{2+} coordinated exclusively to nonmagnetic isotopes, F_n, is

$$F_n = [f(^{16}O) + f(^{18}O)]^n \quad (1)$$

where $f(^{16}O) + f(^{18}O)$ is the fraction of nonmagnetic isotopes. The subtraction procedure involves removing the contribution, F_n, from the composite signal. The signal corresponding to $F_n = 1.0$ is provided by a signal from a concentration-matched sample of unlabeled ligand. This procedure does not require any knowledge of the ^{17}O superhyperfine coupling tensor or of the intrinsic EPR line shapes, because the latter is contained in the spectrum of the unlabeled sample.

Difference spectra are of the form

$$S_d = S_e - F_n S_u \quad (2)$$

where S_d, S_e, and S_u are the signals of the difference spectrum, the experimentally observed spectrum, and the spectrum of the concentration-matched sample with unlabeled ligand, respectively. A value of F_n that is too large results in a negative image of the signal for the unlabeled sample in the resulting difference spectrum, S_d (Reed & Leyh, 1980). If the signals are broad, then it is more difficult to perceive a residual negative image of S_u in difference spectra. This limitation is especially troublesome at higher values of n (Smithers et al., 1990) where small fractions of S_u are subtracted from the

observed signal, S_e. Resolution enhancement of the EPR signals provides a means to improve the contrast in difference spectra corresponding to different values of n.

Resolution Enhancement. Resolution enhancement of the EPR signals was performed by a Fourier method similar to that described by Kauppinen et al. (1981). An analogous procedure for resolution enhancement of EPR spectra was described earlier by Hedberg and Ehrenberg (1968). Fourier transforms of the spectra were deconvoluted with a Lorentzian, $\exp(2\pi\sigma|t|)$ (where σ is the line width), apodized[2] with a squared Bartlett window function, $(1 - |x|/L)^2$ (Kauppinen et al., 1981), and inverse-transformed to the frequency domain. Programs for resolution enhancement were written in interactive FORTRAN and implemented on the VAX platform.

Resolution enhancement is largely an empirical procedure. General prescriptions for resolution enhancement, including guidelines for selection of parameters, are provided in the earlier papers (Hedberg & Ehrenberg, 1968; Kauppinen et al., 1981). Noise is naturally increased by the deconvolution procedure, and the magnitude of this noise is recognized in the "baseline" portions of the spectrum. Truncation of the time-domain data creates "side lobes" that are minimized by the apodization function. The truncation also introduces periodic ($1/L$) noise that is discerned by manipulation of the truncation parameter, L. In complicated spectral patterns, simulation can also aid in distinguishing signal from noise. The "rule-of-thumb" (Kauppinen et al., 1981) that the maximum factor, K, by which signals can be narrowed is $\approx\log$ (S/N) is a reasonable guideline.

Spectral Simulation. To determine the Mn^{2+}–^{17}O superhyperfine coupling constant, signals within the ^{55}Mn hyperfine sextet of the $m_s\ ^1/_2 \leftrightarrow m_s\ ^{-1}/_2$ fine structure transition were simulated with perturbation expressions corrected to third order in the zero-field splitting and ^{55}Mn hyperfine interactions (Markham et al., 1979; Reed & Markham, 1984). The ^{17}O superhyperfine interaction was included as an isotropic term, A_0. Although the ^{17}O superhyperfine coupling comprises both scalar and anisotropic parts, for *ras* p21, the anisotropic dipole–dipole interaction should be erased by rotational averaging.[3] An approximate value for the axial zero-field splitting parameter, D, was available from the previous analysis of the EPR spectrum of *ras* p21–Mn^{II}GDP (Smithers et al., 1990), and the necessity for inclusion of the rhombic parameter, E, was evident in the resolution-enhanced signal of the complex with unlabeled GDP. Values for A_0 and the zero-field splitting parameters D and E were varied in the simulations to achieve an approximate match in the positions of features with those in the experimentally observed signal.

Results

Resolution Enhancement. EPR spectra that had been analyzed previously using the spectral subtraction method (Smithers et al., 1990) were reexamined using a Fourier transform method to enhance the spectral resolution. The EPR spectra obtained from samples containing either water or ^{17}O-enriched water are shown in Figure 1A,B, respectively. The spectra resulting from resolution enhancement of Figure 1A,B are shown as Figure 1C,D, respectively. Following resolution enhancement of the spectrum of the *ras* p21–Mn^{II}GDP complex in ^{17}O-enriched water, the above-mentioned superposition of signals becomes apparent, because a narrow signal (due to Mn^{2+} coordinated to nonmagnetic isotopes of oxygen) can be discerned superimposed on a broader signal (due to Mn^{2+} coordinated to one or more ^{17}O ligands) (Figure 1D). The difference spectrum obtained from the signals in Figure 1A,B when three coordination sites for water ligands are modeled exhibits a slight, but reproducible, anomaly before resolution enhancement (see asterisk in Figure 1E). Following resolution enhancement, the difference spectrum corresponding to three water ligands (Figure 1G) now exhibits a well-defined negative image of the signal in Figure 1C. On the other hand, the difference spectrum obtained when four coordination sites for water ligands are modeled is devoid of the negative image prior to and following resolution enhancement (Figure 1H). The "inflection point" that appears at the center of Figure 1H is expected from resolution enhancement of the signal that corresponds to the sum of signals of ^{17}O-containing species as shown by the simulations in Figure 2. Resolution enhancement thus improves the contrast between the models of three and four water ligands, and the data clearly show that four water molecules are coordinated to Mn^{2+} in the *ras* p21–Mn^{II}GDP complex.

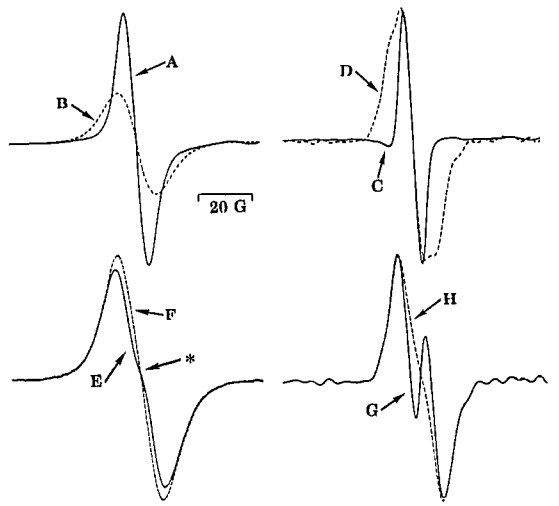

FIGURE 1: Comparison of EPR signals for the *ras* p21–Mn^{II}GDP complex in normal water and in ^{17}O-enriched water, before and after resolution enhancement. (A and B) An overlay of a Mn^{2+} EPR signal (lowest ^{55}Mn hyperfine transition) obtained from a sample in normal water (A) with the EPR signal obtained from a sample in 41% ^{17}O-enriched water (B). (E and F) Difference spectra (see text eq 1 and 2) corresponding to models with three [(E) $F_n = 0.21$] and four [(F) $F_n = 0.12$] coordination sites for water in the complex. The position of the anomaly in curve E is marked with an asterisk. The amplitudes of (E) and (F) [relative to (A) and (B)] have been increased 3-fold. (C, D, G, and H) Spectra resulting from resolution enhancement of signals A, B, E, and F, respectively. The amplitude of (D) [relative to that of (C)] has been increased 5.6-fold, and the amplitudes of (G) and (H) [relative to that of (C)] have been increased 6.8-fold. Samples contained, in buffer A, 30 mg mL^{-1} *ras* $p21_{EJ}$ and 1.0 mM Mn^{2+}. Spectra were recorded at 0 °C. The parameters used for resolution enhancement were $L = 0.220\ G^{-1}$ and $\sigma = 6.06$ G.

Results Using β-^{17}O-Enriched GDP. ^{17}O–Mn^{2+} superhyperfine splitting normally remains unresolved in EPR signals because the linewidths of the signals are larger than the ^{17}O–Mn^{2+} superhyperfine coupling constant. The exceptionally narrow line widths of EPR signals of the *ras* p21–Mn^{II}GDP complex in ^2H_2O (Smithers et al., 1990) prompted an attempt to observe the ^{17}O superhyperfine splitting directly in the EPR signals. The ^{17}O superhyperfine splitting pattern has its simplest form when there is only one ^{17}O ligand in the coordination

[2] Other apodizations were tested (e.g., Gaussian and Hanning) with comparable results.

[3] The principal values of the dipole–dipole coupling tensor, calculated using the point-dipole approximation (Goodman & Raynor, 1970) and a Mn^{2+}–oxygen bond length of 2.1 Å (Sabat et al., 1985), are $T_{xx} = T_{yy} = +0.2$ G and $T_{zz} = -0.4$ G. For *ras* p21, the rotational correlation time, τ_r, at 0 °C is $\sim 1.4 \times 10^{-8}$ s. The anisotropy of 0.6 G (1.06×10^7 rad s^{-1}) in the superhyperfine interaction should be erased by rotational averaging (i.e., $\Delta\omega\tau_r \cong 0.15$).

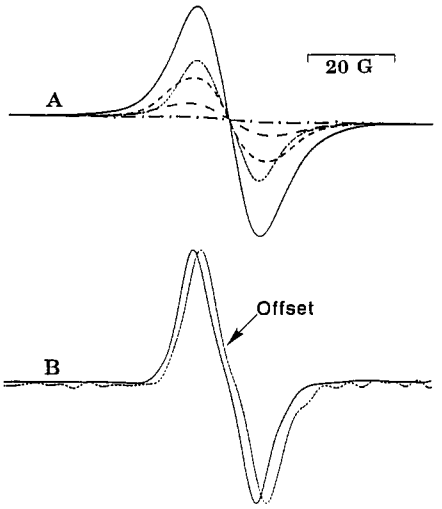

FIGURE 2: Simulation of the expected difference spectrum, if four water molecules are coordinated to Mn^{2+}. (A) Overlay of the expected spectral contributions from Mn^{2+} in coordination shells containing one (···), two (- - -), three (– –), and four (–·–) ^{17}O-containing water molecules and the sum (—) of these contributions. The simulated spectra were constructed from the actual EPR spectrum (Figure 1A) by assuming an isotropic superhyperfine coupling constant of 2.4 G. The probability (relative weight) of each subsignal corresponding to different numbers of ^{17}O ligands was calculated with $f(^{17}O) = 0.41$. (B) Comparison of the simulated spectrum (solid line above) after resolution enhancement with the actual resolution-enhanced difference spectrum (dashed line) that was shown as in Figure 1H. The two signals are offset on the abscissa by 2 G. The parameters used for resolution enhancement were $L = 0.220$ G^{-1} and $\sigma = 6.06$ G.

sphere. The β-phosphate group of GDP had been identified as a ligand in an earlier EPR study (Feuerstein et al., 1987), and this ligand could therefore be used to introduce a single ^{17}O into the coordination sphere of Mn^{2+} in the *ras* p21–$Mn^{II}GDP$ complex.

A relatively low field modulation amplitude (1.4 G) was employed in recording of the experimental spectra to lower the instrumental barrier to resolution. Signals from the lowest field ^{55}Mn hyperfine transition of samples with unlabeled GDP and with β-^{17}O-enriched GDP were recorded (see Figure 3A) by scan-averaging to compensate for degradation of S/N resulting from the low modulation amplitudes. The EPR signal of the enriched sample (Figure 3A, dashed curve) consists of a superposition of a signal, S_u, of Mn^{2+} bound to the nonmagnetic isotopes of oxygen, and a signal of Mn^{2+} bound to ^{17}O. The contribution from the latter is obscured by this superposition of the signal F_nS_u. Thus, F_nS_u is removed from the experimentally observed spectrum using the spectral subtraction method (eq 1 and 2). An ^{17}O enrichment in the β-phosphate of GDP of 36 ± 1% was determined through this subtraction operation.

There is a hint of ^{17}O superhyperfine splitting in the signal, S_d, from Mn^{2+} bound to an ^{17}O in the β-phosphate of GDP before resolution enhancement as shown in Figure 3B. The ^{17}O superhyperfine splitting is evident following modest resolution enhancement of the signal as shown in Figure 4A. The signal is asymmetric, and this asymmetry is accentuated at a higher level of resolution enhancement (Figure 4B). The parent ^{55}Mn hyperfine transition contains anisotropy due to second-order terms in the zero-field splitting interaction (Reed & Markham, 1984). The D (113 G) and E (31 G) terms of the zero-field splitting interaction were modeled by simulation of the corresponding transition in the resolution-enhanced spectrum of the sample of unlabeled GDP (see Experimental Procedures). Inclusion of an isotropic ^{17}O superhyperfine coupling in the simulation (Figure 4C) approximates the

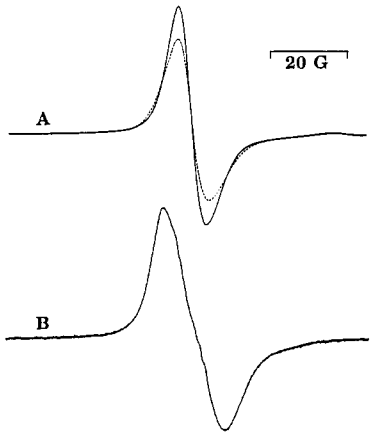

FIGURE 3: Comparison of EPR signals of *ras* p21–$Mn^{II}[\beta$-$^{17}O]GDP$ and *ras* p21–$Mn^{II}GDP$. (A) Overlay of the EPR signal (lowest field ^{55}Mn hyperfine transition) obtained from a sample of the *ras* p21–$Mn^{II}GDP$ complex with unlabeled GDP (solid line) with the signal obtained from a concentration-matched sample containing [β-^{17}O]-enriched GDP (dashed line). (B) Diffrence spectrum obtained following subtraction of 64% of the signal of unlabeled GDP from the signal of the ^{17}O-enriched sample ($F_n = 0.64$, see text eq 1 and 2). The final concentrations in the EPR samples were 2.4 mM *ras* p21, 36 mM nucleotide, and 1.7 mM Mn^{2+}. The EPR signal of each sample was obtained by accumulating 64 4-min scans with a 1.4-G field modulation. The amplitude of (B) has been increased 6.8-fold relative to the amplitude of (A).

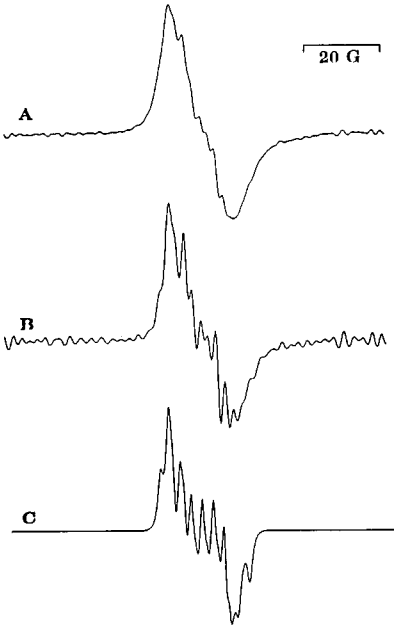

FIGURE 4: Resolution enhancement and simulation of the EPR signal from the *ras* p21–$Mn^{II}[\beta$-$^{17}O]GDP$ complex. (A) Resolution-enhanced EPR signal from Figure 3B with parameters $L = 0.62$ G^{-1} and $\sigma = 1.73$ G. (B) Resolution enhancement with parameters $L = 0.55$ G^{-1} and $\sigma = 2.60$ G. (C) Simulation of (B) using $D = 113$ G $E = 31$ G, $A_0 = 2.9$ G, and line width of 0.8 G. Ten thousand crystal orientations were sampled in the powder simulation.

positions of the superhyperfine features in the signal. The isotropic coupling constant, $|A_0| = 2.9 \pm 0.1$ G, is obtained from the simulation.

Discussion

The spectroscopic results obtained from the *ras* p21–$Mn^{II}GDP$ complex in solution establish the presence of four water molecules in the first coordination sphere of Mn^{2+}. This conclusion agrees with the X-ray crystallographic results (Milburn et al., 1990; Tong et al., 1991) obtained from studies of crystals of the $Mg^{II}GDP$ complex wherein Asp-57 is a

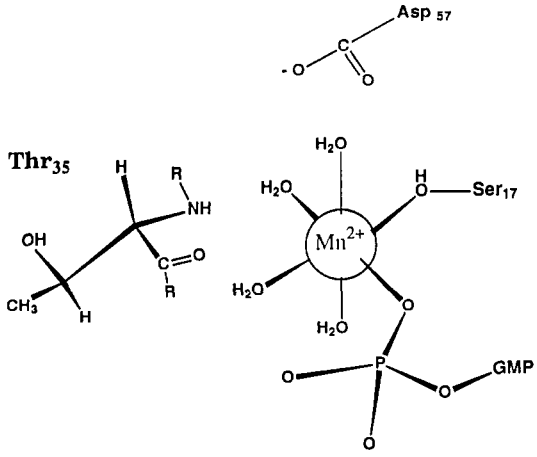

FIGURE 5: Schematic view of the MnGDP complex bound to the *ras* p21 protein. The positions of amino acid residues are taken from the X-ray crystallographic structure (Milburn et al., 1990; Tong et al., 1991).

second-sphere ligand. A schematic view of the complex is given in Figure 5. Wittinghofer and Pai (1991) have suggested that the disagreement regarding the liganding of Asp-57 in the $Mg^{II}GDP$ complex with *ras* p21 may be ascribed either to the differences in crystallization conditions or to uncertainties in electron densities obtained from diffraction from the photolyzed crystals. They also suggest that the structure of the complex may differ with different species (e.g., Mn^{2+} and Ca^{2+}) of divalent metal ions at the nucleotide site. Mn^{2+} has a larger ionic radius than Mg^{2+}, but one would expect this size difference to ease access of Asp-57 to the primary coordination shell of Mn^{2+}, if this ligand exchange were to occur. Moreover, the agreement between the spectroscopic results for solution of the *ras* p21–$Mn^{II}GDP$ complex and the crystallographic results on the *ras* p21–$Mg^{II}GDP$ complex (Milburn et al., 1990; Tong et al., 1991) indicates that the Mn^{2+}-for-Mg^{2+} substitution is likely isomorphous in this protein–nucleotide complex.

The nucleotide binding cassettes in several other proteins (Fry et al., 1986) contain an Asp residue in a position analogous to the location Asp-57 of *ras* p21. Although Asp-57 is not a first-sphere ligand to the metal ion in *ras* p21, there is early evidence which suggests that liganding of the carboxylate from this residue in the nucleotide binding cassette may be a "local option" among the individual species of protein. For example, evidence from site-directed mutagenesis and NMR spectroscopy of adenylate kinase suggests that Asp-93 interacts with Mg^{2+} in the active site of the enzyme (Yan & Tsai, 1991). The distinct possibility of structural diversity within these seemingly homologous nucleotide binding sites suggests a cautious approach to assigning structural details by analogy.

The resolution enhancement methods that are applied in this work facilitate quantitation of the EPR data and permit detection of features that are hidden in the original envelope of overlapping transitions. Hyde et al. (1992) have recently discussed strategies for resolution enhancement of EPR spectra. Resolution enhancement should be considered in EPR spectroscopy whenever S/N in the data can be sacrificed for more accurate information on line positions.

ACKNOWLEDGMENTS

We are grateful to Dr. George D. Markham for providing data acquisition software and to Dr. Gary Wesenberg and Mr. Kenneth C. Johnson for assistance with computer programming and interfacing.

REFERENCES

Ames, G. F.-L. (1986) *Annu. Rev. Biochem. 55*, 397–425.
Barbacid, M. (1987) *Annu. Rev. Biochem. 56*, 779–827.
Eccleston, J. F., Webb, M. R., Ash, D.E., & Reed, G. H. (1981) *J. Biol. Chem. 256*, 10774–10777.
Ellis, R. W., Lowry, D. R., & Scolnick, E. M. (1982) *Adv. Viral Oncol. 1*, 107–126.
Feuerstein, J., Kalbitzer, H. R., John, J., Goody, R. S., & Wittinghofer, A. (1987) *Eur. J. Biochem. 162*, 49–55.
Fry, D. C., Kuby, S. A., & Mildvan, A. S. (1986) *Proc. Natl. Acad. Sci. U.S.A. 83*, 907–911.
Gibbs, J. B., Sigal, I. S., Poe, M., & Scolnick, E. M. (1984) *Proc. Natl. Acad. Sci. U.S.A. 81*, 5704–5708.
Goodman, B. A., & Raynor, J. B. (1970) *Adv. Inorg. Chem. Radiochem. 13*, 135–362.
Hall, A. (1990) *Science 249*, 635–640.
Hedberg, A., & Ehrenberg, A. (1968) *J. Chem. Phys. 48*, 4822–4828.
Hyde, J. S., Jesmanowicz, A., Ratke, J. J., & Antholine, W. E. (1992) *J. Magn. Reson. 96*, 1–13.
Hyde, S. C., Emsley, P., Hartshorn, M. J., Mimmack, M. M., Gileadi, U., Pearce, S. R., Gallagher, M. P., Gill, D. R., Hubbard, R. E., & Higgins, C. F. (1990) *Nature 346*, 362–365.
Kauppinen, J. K., Moffatt, D. J., Mantsch, H. H., & Cameron, D. G. (1981) *Appl. Spectrosc. 35*, 271–276.
Lodato, D. T., & Reed, G. H. (1987) *Biochemistry 26*, 2243–2250.
Markham, G. D., Nageswara Rao, B. D., & Reed, G. H. (1979) *J. Magn. Reson. 33*, 595–602.
Milburn, M. V., Tong, L., de Vos, A. M., Brunger, A., Yamaizumi, Z., Nishimura, S., & Kim, S.-H. (1990) *Science 247*, 939–945.
Pai, E. F., Kabsch, W., Krengel, U., Holmes, K. C., John, J., & Wittinghofer, A. (1989) *Nature 341*, 209–214.
Pai, E. F., Krengel, U., Petsko, G. A., Goody, R. S., Kabsch, W., & Wittinghofer, A. (1990) *EMBO J. 9*, 2351–2359.
Reed, G. H., & Leyh, T. S. (1980) *Biochemistry 19*, 5472–5480.
Reed, G. H., & Markham, G. D. (1984) *Biol. Magn. Reson. 6*, 73–142.
Sabat, M., Cini, R., Haromy, T., & Sundaralingam, M. (1985) *Biochemistry 24*, 7827–7833.
Schlichting, I., Almo, S. C., Rapp, G., Wilson, K., Petratos, K., Lentfer, A., Wittinghofer, A., Kabsch, W., Pai, E. F., Petsko, G. A., & Goody, R. S. (1990) *Nature 345*, 309–315.
Smithers, G. W., Poe, M., Latwesen, D. G., & Reed, G. H. (1990) *Arch. Biochem. Biophys. 280*, 416–420.
Tong, L., de Vos, A. M., Milburn, M. V., & Kim, S.-H. (1991) *J. Mol. Biol. 217*, 503–516.
Wittinghofer, A., & Pai, E. F. (1991) *Trends Biochem. Sci. 16*, 382–387.
Yan, H., & Tsai, M.-D. (1991) *Biochemistry 30*, 5539–5546.